Chapter 7
Answers to Problems

7.1 In I_h all *d* orbitals transform as the species H_g. Therefore they remain degenerate. All degenerate *d* orbitals will rise in energy due to electron-electron repulsions between the metal and "ligand" C_{60}.

7.2 See J. J. Zuckerman, *J. Chem Educ.*, **1965**, *42*, 315 and R. Krishnamurthy and W. B. Schaap, *J. Chem. Educ.*, **1969**, *46*, 799.

(a) ML_2 - linear ($D_{\infty h}$)

___ $\sigma_g^+ d_{z^2}$
___ ___ $\pi_g d_{xz}, d_{yz}$
___ ___ $\delta_g d_{x^2-y^2}, d_{xy}$

(b) ML_3 - trigonal planar (D_{3h})

___ ___ $e' d_{x^2-y^2}, d_{xy}$
___ $a_1' d_{z^2}$
___ ___ $e'' d_{xz}, d_{yz}$

(c) ML_5 - trigonal bipyramid (D_{3h})

___ $a_1' d_{z^2}$
___ ___ $e' d_{x^2-y^2}, d_{xy}$
___ ___ $e'' d_{xz}, d_{yz}$

(d) ML_5 - square pyramid (C_{4v})

___ $b_1 d_{x^2-y^2}$
___ $a_1 d_{z^2}$
___ $b_2 d_{xy}$
___ ___ $e d_{xz}, d_{yz}$

(e) ML_6 - trigonal antiprism (D_{3d})

___ ___ $e_g d_{xz}, d_{yz}$
___ ___ $e_g d_{x^2-y^2}, d_{xy}$
___ $a_{1g} d_{z^2}$

(f) ML_7 - capped trigonal prism (C_{2v}) The order of the orbitals is not unambiguous in this case and will depend upon the details of the geometry. The ordering suggested below is based on the following idealized model, in which the central atom lies in the plane of the four ligand atoms from which the capped position emerges.

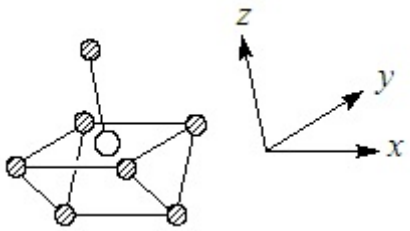

___ $a_2\ d_{xy}$
___ $a_1\ d_{z^2}$
___ $b_1\ d_{xz}$
___ $a_1\ d_{x^2-y^2}$
___ $b_2\ d_{yz}$

(g) ML_7 - pentagonal bipyramid (D_{5h})

___ $a_1'\ d_{z^2}$
___ ___ $e_2'\ d_{x^2-y^2}, d_{xy}$
___ ___ $e_1''\ d_{xz}, d_{yz}$

(h) ML_8 - square antiprism (D_{4d})

___ ___ $e_3\ d_{xz}, d_{yz}$
___ ___ $e_2\ d_{x^2-y^2}, d_{xy}$
___ $a_1\ d_{z^2}$

(i) ML_8 - cubic (O_h) Same splitting as an octahedron, but with reversed order.

___ ___ ___ $t_{2g}\ d_{xz}, d_{yz}, d_{xy}$
___ ___ $e_g\ d_{x^2-y^2}, d_{z^2}$

(j) ML_9 - tricapped trigonal prism (D_{3h})

___ ___ $e''\ d_{xz}, d_{yz}$
___ ___ $e'\ d_{x^2-y^2}, d_{xy}$
___ $a_1'\ d_{z^2}$

7.3 One way of approaching this to consider an initial tetragonal distortion, involving stretching along z, followed by compression along x to give the orthorhombically distorted structure; i.e., $O_h \rightarrow D_{4h} \rightarrow D_{2h}$. This would lead to the following CFT orbital splitting diagram:

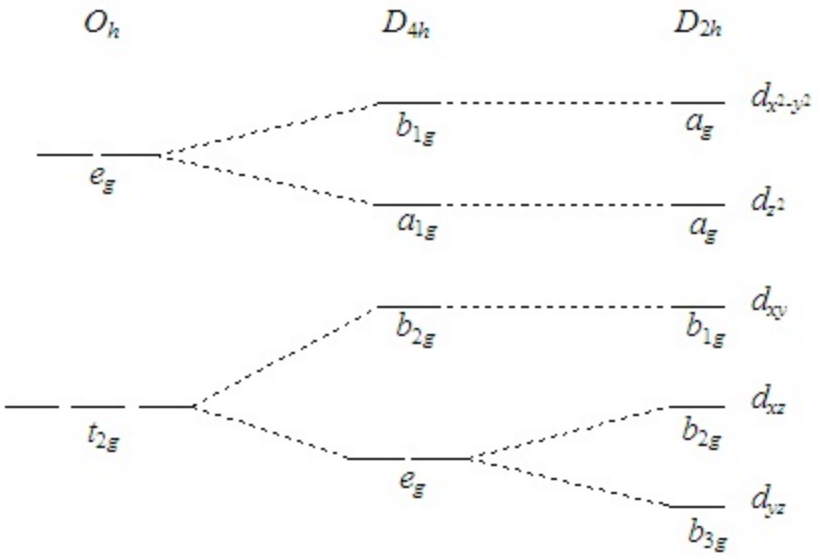

As a result of the orthorhombic distortion, orbitals with an x component will rise in energy, while those with a z component will fall in energy. Relative to the D_{4h} z-stretch case, the separation between $d_{x^2-y^2}$ and d_{z^2} orbitals will increase, as will that between the d_{xy} and d_{xz} orbitals. The degeneracy between d_{xz} and d_{yz} in D_{4h} (e_g) will be lifted in D_{2h} as the d_{yz} orbital becomes more stable.

This is an allowed Jahn-Teller distortion, because D_{2h} is centrosymmetric, as is O_h. For example, for d^1 the proposed orthorhombic distortion would give a nondegenerate ground state. This distortion would be more likely than a tetragonal z-stretch (which leads to a doubly degenerate ground state), but it is no more likely than a tetragonal z-compression (which leads to a nondegenerate state). As always, we cannot predict the nature of the distortion that will occur on the basis of the Jahn-Teller theorem.

7.4 Using the C_3 axis shown below, clockwise rotations will result in the transformations listed in the following table.

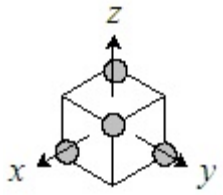

	C_3	C_3^2
x	z	y
y	x	z
z	y	x
d_{xy}	d_{zx}	d_{yz}
d_{yz}	d_{zy}	d_{yx}
d_{yz}	d_{xy}	d_{zx}
$d_{x^2-y^2}$	$d_{z^2-x^2}$	$d_{y^2-z^2}$
$d_{2z^2-x^2-y^2}$	$d_{2y^2-z^2-x^2}$	$d_{2x^2-y^2-z^2}$

The first three rows of *d* orbital listings show the equivalence of the orbitals comprising the t_2 set. The last two lines show the equivalence of the orbitals comprising the *e* set, when the transformed orbitals are seen to be related to $d_{x^2-y^2}$ and $d_{2z^2-x^2-y^2}$ by Eqs. (7.1a) - (7.1d).

7.5 Taking the functions $d_{x^2-y^2}$, $d_{z^2-x^2}$, and $d_{z^2-y^2}$ as reference functions, C_8 rotations about an axis perpendicular to the plane of the cloverleaf in each case (z, y, and x) will effect transformations to d_{xy}, d_{xz}, and d_{yz}, respectively. The interconversion of $d_{x^2-y^2}$ and d_{xy} is shown below.

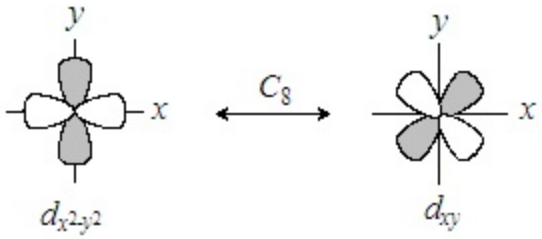

As noted in the statement of the problem, $d_{z^2-x^2}$ and $d_{z^2-y^2}$ can be combined into the conventional function for d_{z^2}. As a result, the operations of $C_8(z)$, $C_8(y)$, and $C_8(x)$ would interconvert all five conventional *d* orbitals into each other or the components of the combination that makes up d_{z^2}, making them degenerate with each other. Of course, C_8 is not an operation in O_h, and the five *d* orbitals cannot be made completely degenerate by any operation in that point group.

7.6 (a) D_{3h}

$\chi(E) = 2l + 1 = 5$

$\chi(C_3) = \{\sin (2.5)(120^o)\}/\{\sin 60^o\} = -0.866/0.866 = -1$

$\chi(C_2) = \{\sin (2.5)(180^o)\}/\{\sin 90^o\} = 1/1 = 1$

$\chi(\sigma) = + \sin \{(2.5)(180^o)\} = 1$

$\chi(S_3) = + \{\sin (2.5)(120^0 + 180^o)\}/\{\sin 150^o\} = 0.5/0.5 = 1$

D_{3h}	E	$2C_3$	$3C_2$	σ_h	$2S_3$	$3\sigma_v$
Γ_d	5	-1	1	1	1	1

$$\Gamma_d = A_1' + E' + E''$$

(b) D_{2h}

$\chi(E) = 2l + 1 = 5$

$\chi(C_2) = \{\sin (2.5)(180^o)\}/\{\sin 90^o\} = 1/1 = 1$

$\chi(i) = + \{2l + 1) = 5$

$\chi(\sigma) = + \sin \{(2.5)(180^o)\} = 1$

D_{2h}	E	$C_2(z)$	$C_2(y)$	$C_2(x)$	i	$\sigma(xy)$	$\sigma(xz)$	$\sigma(yz)$
Γ_d	5	1	1	1	5	1	1	1

$$\Gamma_d = 2A_g + B_{1g} + B_{2g} + B_{3g}$$

(c) C_{4v}

$\chi(E) = 2l + 1 = 5$

$\chi(C_4) = \{\sin (2.5)(90^o)\}/\{\sin 45^o\} = -0.707/0.707 = -1$

$\chi(C_2) = \{\sin (2.5)(180^o)\}/\{\sin 90^o\} = 1/1 = 1$

$\chi(\sigma) = + \sin \{(2.5)(180^o)\} = 1$

C_{4v}	E	$2C_4$	C_2	$2\sigma_v$	$2\sigma_d$
Γ_d	5	-1	1	1	1

$$\Gamma_d = A_1 + B_1 + B_2 + E$$

(d) I

$\chi(E) = 2l + 1 = 5$

$\chi(C_5) = \{\sin (2.5)(72^o)\}/\{\sin 36^o\} = 0/0.588 = 0$

$\chi(C_5^2) = \{\sin (2.5)(144^o)\}/\{\sin 72^o\} = 0/0.951 = 0$

$\chi(C_3) = \{\sin (2.5)(120^o)\}/\{\sin 60^o\} = -0.866/0.866 = -1$

$\chi(C_2) = \{\sin (2.5)(180^o)\}/\{\sin 90^o\} = 1/1 = 1$

I_h	E	$12C_5$	$12C_5^2$	$20C_3$	$15C_2$
Γ_d	5	0	0	-1	1

$$\Gamma_d = H \Rightarrow H_g \text{ in } I_h$$

7.7 With $l = 3$, f orbitals are inherently *ungerade*, requiring the use of the negative sign with Eqs. (7.4) - (7.6).

(a) T_d

$\chi(E) = 2l + 1 = 7$

$\chi(C_3) = \{\sin (3.5)(120^o)\}/\{\sin 60^o\} = 0.866/0.866 = 1$

$\chi(C_2) = \{\sin (3.5)(180^o)\}/\{\sin 90^o\} = -1/1 = -1$

$\chi(S_4) = - \{\sin (3.5)(270^o)\}/\{\sin 135^o\} = -(-0.707)/0.707 = 1$

$\chi(\sigma) = - \sin \{(3.5)(180^o)\} = - (-1) = 1$

T_d	E	$8C_3$	$3C_2$	$6S_4$	$6\sigma_d$
Γ_f	7	1	-1	1	1

$$\Gamma_f = A_1 + T_1 + T_2$$

(b) O_h. By correlation of the T_d results obtained in part (a) to the corresponding *ungerade* species of O_h we obtain

$$\begin{aligned} T_d &\rightarrow O_h \\ A_1 &\rightarrow A_{2u} \\ T_1 &\rightarrow T_{2u} \\ T_2 &\rightarrow T_{1u} \end{aligned}$$

Alternately, the reducible representation can be generated and decomposed in the usual way.

$\chi(E) = 2l + 1 = 7$
$\chi(C_3) = \{\sin (3.5)(120^o)\}/\{\sin 60^o\} = 0.866/0.866 = 1$
$\chi(C_2) = \{\sin (3.5)(180^o)\}/\{\sin 90^o\} = -1/1 = -1$
$\chi(C_4) = \{\sin (3.5)(90^o)\}/\{\sin 45^o\} = -0.707/0.707 = -1$
$\chi(i) = -(2l + 1) = -7$
$\chi(S_4) = -\{\sin (3.5)(270^o)\}/\{\sin 135^o\} = -(-0.707)/0.707 = 1$
$\chi(S_6) = -\{\sin (3.5)(240^o)\}/\{\sin 120^o\} = -(0.866)/0.866 = -1$
$\chi(\sigma) = -\sin\{(3.5)(180^o)\} = -(-1) = 1$

O_h	E	$8C_3$	$6C_2$	$6C_4$	$3C_2$	i	$6S_4$	$8S_6$	$3\sigma_h$	$6\sigma_d$
Γ_f	7	1	-1	-1	-1	-7	1	-1	1	1

$$\Gamma_f = A_{2u} + T_{1u} + T_{2u}$$

(c) D_{4h}. By correlation of the O_h results obtained in part (b) to the corresponding *ungerade* species D_{4h} of we obtain

$$\begin{aligned} O_h &\rightarrow D_{4h} \\ A_{2u} &\rightarrow B_{1u} \\ T_{2u} &\rightarrow A_{2u} + E_u \\ T_{1u} &\rightarrow B_{2u} + E_u \end{aligned}$$

Alternately, the reducible representation can be generated and decomposed in the usual way.

$\chi(E) = 2l + 1 = 7$
$\chi(C_4) = \{\sin (3.5)(90^o)\}/\{\sin 45^o\} = -0.707/0.707 = -1$
$\chi(C_2) = \{\sin (3.5)(180^o)\}/\{\sin 90^o\} = -1/1 = -1$
$\chi(i) = -(2l + 1) = -7$
$\chi(S_4) = -\{\sin (3.5)(270^o)\}/\{\sin 135^o\} = -(-0.707)/0.707 = 1$
$\chi(\sigma) = -\sin\{(3.5)(180^o)\} = -(-1) = 1$

D_{4h}	E	$2C_4$	C_2	$2C_2'$	$2C_2''$	i	$2S_4$	σ_h	$2\sigma_v$	$2\sigma_d$
Γ_f	7	-1	-1	-1	-1	-7	1	1	1	1

$$\Gamma_f = A_{2u} + B_{1u} + B_{2u} + 2E_u$$

(d) D_{3d}. By correlation of the O_h results obtained in part (b) to the corresponding *ungerade* species D_{4h} of we obtain

$$\begin{aligned} O_h &\rightarrow D_{3d} \\ A_{2u} &\rightarrow A_{2u} \\ T_{2u} &\rightarrow A_{2u} + E_u \\ T_{1u} &\rightarrow A_{1u} + E_u \end{aligned}$$

Alternately, the reducible representation can be generated and decomposed in the usual way.

$\chi(E) = 2l + 1 = 7$
$\chi(C_3) = \{\sin (3.5)(120^o)\}/\{\sin 60^o\} = 0.866/0.866 = 1$
$\chi(C_2) = \{\sin (3.5)(180^o)\}/\{\sin 90^o\} = -1/1 = -1$
$\chi(i) = -(2l + 1) = -7$
$\chi(S_6) = -\{\sin (3.5)(240^o)\}/\{\sin 120^o\} = -(0.866)/0.866 = -1$
$\chi(\sigma) = -\sin\{(3.5)(180^o)\} = -(-1) = 1$

D_{3d}	E	$2C_3$	$3C_2$	i	$2S_6$	$3\sigma_d$
Γ_f	7	1	-1	-7	-1	1

$$\Gamma_f = A_{1u} + 2A_{2u} + 2E_u$$

7.8 (a) Only degenerate states are subject to Jahn-Teller distortions. Assuming the ordering of *d* orbitals shown on the extreme right of Fig. 7.9, only the configurations d^1 and d^3 result in degenerate ground states and would be distorted. If the e_g orbitals are above the a_{1g} orbital, the ground state configurations d^3 and d^5 would be degenerate and would be distorted. Of course, any excited states in which one or three electrons occupy the e_g orbitals would also be degenerate and result in Jahn-Teller distortions.

(b) D_{4h} is a centrosymmetric point group, so any Jahn-Teller distortion would produce a centrosymmetric structure. Disregarding ligand structure, the only centrosymmetric subgroups are D_{2h} and C_i. A D_{2h} structure would result from shortening or lengthening a *trans*-related pair of bonds relative to the other pair of *trans*-related bonds. If the L–M–L' bond angle in such a structure were distorted from 90°, the symmetry would descend further to C_i. As always with the Jahn-Teller theorem, the precise distortion cannot be predicted.

(c) Almost all ML_4 D_{4h} complexes are $d^{7\text{-}8}$, in which the e_g orbitals are filled, regardless of their relative order with the a_{1g} orbital. Consequently, square planar complexes have nondegenerate ground states and are immune to Jahn-Teller distortions.

7.9 (a) As shown for PF_5 (cf. problem 4.13), for the ligand σ-SALCs, $\Gamma = 2A_1' + E' + A_2''$. The symmetries of the *d* orbitals, taken from the direct product transformations in D_{3h}, are $d_{z^2} = A_1'$, $(d_{x^2-y^2}, d_{xy}) = E'$, $(d_{xz}, d_{yz}) = E''$. Bonding and antibonding combinations can be formed with A_1' and E' symmetries, but the E'' symmetry (d_{xz}, d_{yz}) pair must be nonbonding in this model. The following qualitative MO can be constructed.

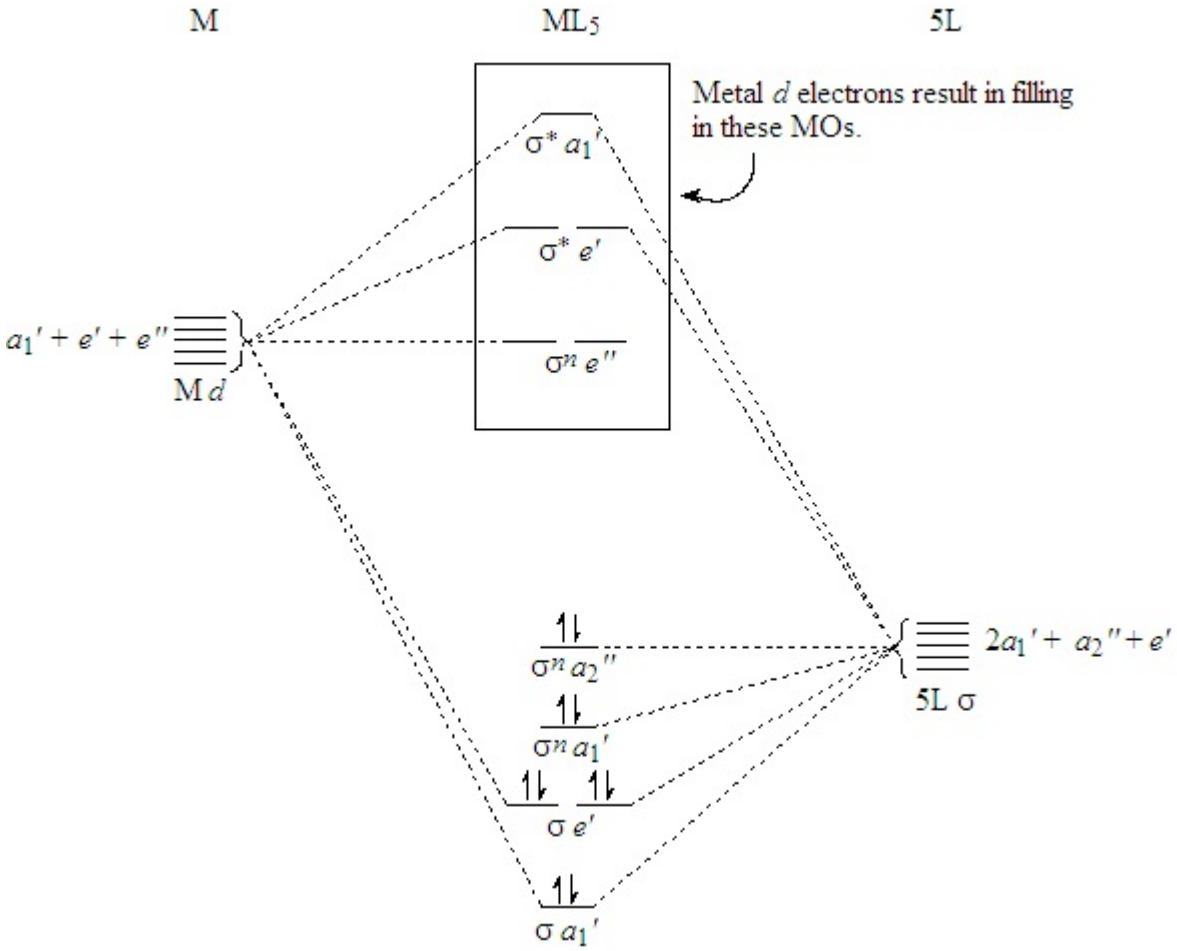

(b) The upper three levels (boxed region, above) have identical splitting to that in the CFT *tbp* model (cf. problem 7.2 c). Electron pairs contributed by the ligands are sufficient to fill all lower levels. Therefore, any electrons contributed by the metal ion result in filling in the upper three levels, in the same manner as predicted in the CFT model.

(c) The a_1' combination with the d_{z^2} orbital would use opposite signs for the axial and equatorial ligand σ AOs. The SALC would be $\Phi_1 = 1/\sqrt{5}\{\phi_1 + \phi_2 + \phi_3 - \phi_4 - \phi_5\}$. The resulting LCAO would be:

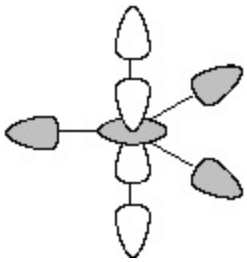

The two e' SALCs, which combine with $d_{x^2-y^2}$ and d_{xy}, involve only equatorial functions. They are $\Phi_2 = 1/\sqrt{6}\{2\phi_1 - \phi_2 - \phi_3\}$ and $\Phi_3 = 1/\sqrt{2}\{\phi_2 - \phi_3\}$, respectively. The resulting LCAOs, projected in the *xy* plane, would be:

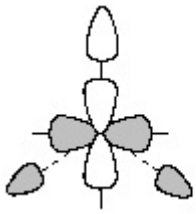

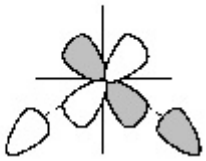

(d) The a_1' and a_2'' SALCs, which form nonbonding MOs in the *d*-only scheme, could form bonding and antibonding combinations with *s* and p_z AOs on the metal. The p_x and p_y AOs could form bonding and antibonding combinations with the e' SALCs, which in the *d*-only scheme form bonding and antibonding combinations with $d_{x^2-y^2}$ and d_{xy} AOs. This competition would result in six mixed MOs of varying bonding, nonbonding, and antibonding character, depending upon the relative contributions of *d* and *p* AOs.

7.10 (a) The representation of σ-SALCs is based on the following model:

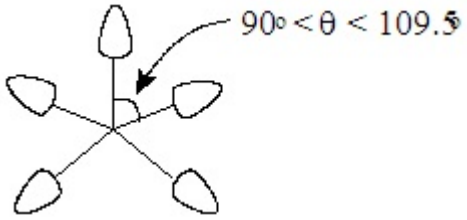

C_{4v}	E	$2C_4$	C_2	$2\sigma_v$	$2\sigma_d$
Γ_σ	5	1	1	3	1

$$\Gamma_\sigma = 2A_1 + B_1 + E$$

The AO symmetries of the central M atom are shown below.

$$(n-1)d: \quad d_{z^2} = A_1,\ d_{x^2-y^2} = B_1,\ d_{xy} = B_2,\ (d_{xz}, d_{yz}) = E$$

$$ns: \quad s = A_1$$

$$np: \quad p_z = A_1,\ (p_x, p_y) = E$$

The d_{xy} orbital (b_2) has no symmetry match with a SALC and must remain nonbonding.

(b) For simplicity, the following sketches show θ = 90°. The three kinds of potentially bonding interactions between $(n-1)d$ orbitals and σ-SALCs are the following:

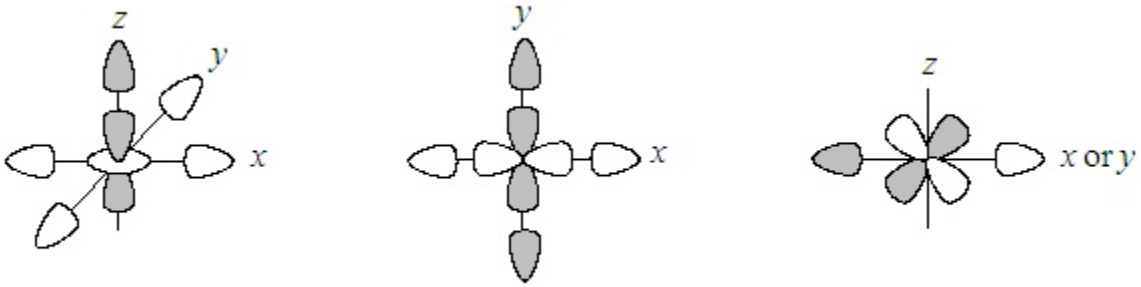

a_1 (z^2) $\qquad$ b_1 (x^2-y^2) $\qquad$ e (xz, yz)

The e (xz, yz) combinations are nonbonding at θ = 90° and become only slightly bonding with θ > 90°. A better bonding combination with the E SALCs can be formed with p_x and p_y AOs (see below).

The *ns* and *np* AOs can form the following bonding combinations:

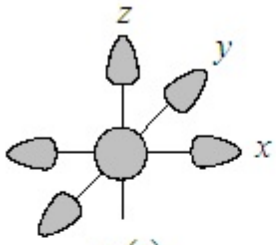

a_1 (*s*)

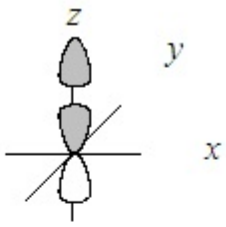

a_1 (*z*)

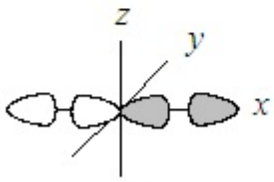

e (*x*)

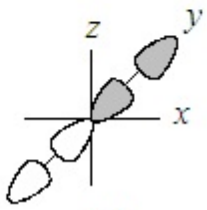

e (*y*)

The *ns* and *np* combinations for a_1 are probably mixed. With a total of three a_1 AOs (d_{z^2}, *s*, p_z) and two a_1 SALCs, there can be only five MOs. We will assume bonding and antibonding combinations for d_{z^2} (a_1) and *s* (a_1), and treat p_z (a_1) as essentially nonbonding. The two *e* combinations with p_x and p_y have better overlap with the *E* SALCs than d_{xz} and d_{yz}. Therefore we will form bonding and antibonding combinations with these and assume that the d_{xz} and d_{yz} orbitals are essentially nonbonding.

(c) The following MO scheme is based on the assumptions noted above.

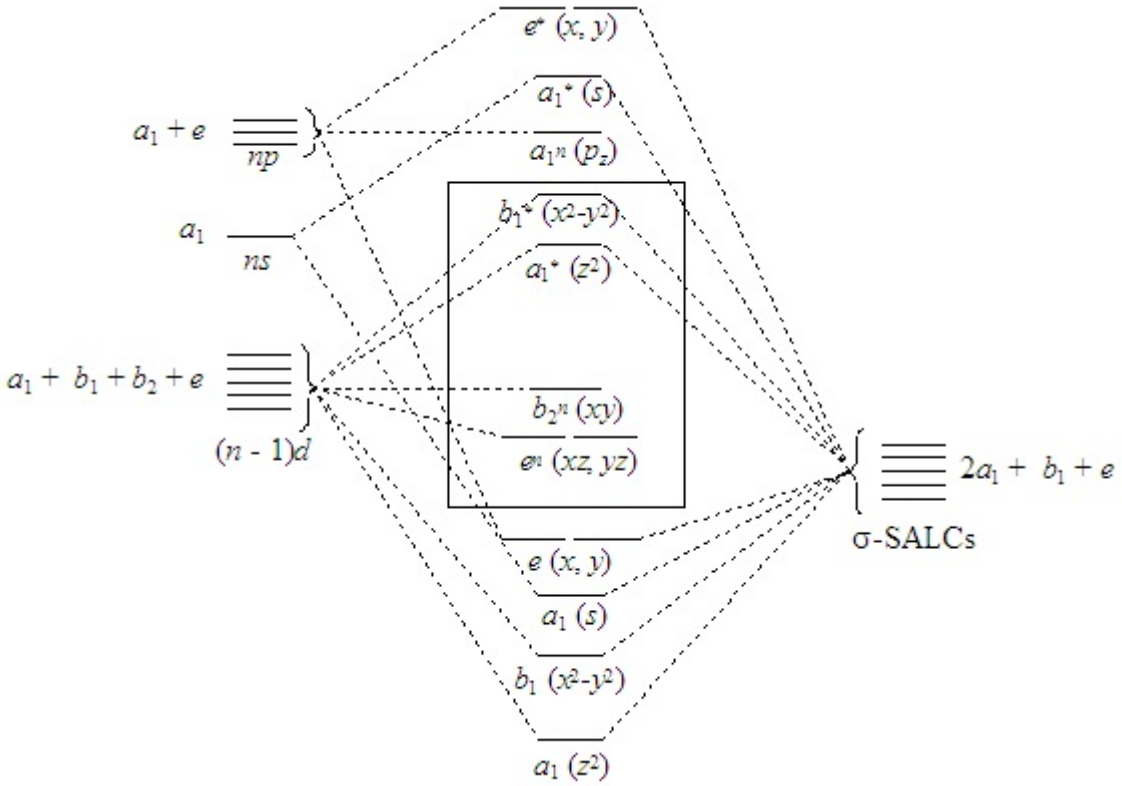

(d) In the MO scheme shown for part (c), electrons from ligand would fill all levels below those in the box. The MOs in the box have the same symmetries and are in the same relative energy order as the *d* orbitals in a square pyramidal crystal field [cf. answer to 7.2 (d)]. Thus, the filling of electrons in MOs above the four lowest bonding levels is equivalent to the presumed filling of electrons in *d* orbitals of the CFT model.

7.11 (a) The SALCs are identical to the oxygen σ- and π-SALCs derived for CO_2 in Chapter 4 (pp. 118-126). Thus,

$$\Gamma_\sigma = \Sigma_g^+ + \Sigma_u^+$$
$$\Gamma_\pi = \Pi_u + \Pi_g$$

(b) Assuming *p* orbitals on the ligands, the SALCs would have the following forms:

Σ_g^+  Σ_u^+ 

Π_u   both *xz* and *yz* planes

Π_g   both *xz* and *yz* planes

The normalized wave function expressions for these SALCS are as follows:

$$\Sigma_g^+ = 1/\sqrt{2}\{\phi_z(1) + \phi_z(2)\} \qquad \Sigma_u^+ = 1/\sqrt{2}\{\phi_z(1) - \phi_z(2)\}$$

$$\Pi_u(x) = 1/\sqrt{2}\{\phi_x(1) + \phi_x(2)\} \qquad \Pi_u(y) = 1/\sqrt{2}\{\phi_y(1) + \phi_y(2)\}$$

$$\Pi_g(x) = 1/\sqrt{2}\{\phi_x(1) - \phi_x(2)\} \qquad \Pi_g(y) = 1/\sqrt{2}\{\phi_y(1) - \phi_y(2)\}$$

(c) $s = \Sigma_g^+ \Rightarrow$ bonding and antibonding with Σ_g^+ SALC

$p_z = \Sigma_u^+ \Rightarrow$ bonding and antibonding with Σ_u^+ SALC

$(p_x, p_y) = \Pi_u \Rightarrow$ bonding and antibonding with Π_u SALCs

$d_{z^2} = \Sigma_g^+ \Rightarrow$ bonding and antibonding with Σ_g^+ SALC

$(d_{xz}, d_{yz}) = \Pi_g \Rightarrow$ bonding and antibonding with Π_g SALCs

$(d_{x^2-y^2}, d_{xy}) = \Delta_g \Rightarrow$ nonbonding.

(d) Both *ns* and $(n - 1)d_{z^2}$ AOs can form bonding and antibonding combinations with the Σ_g^+ SALC, so *s-d* mixing is possible. Being higher in energy, the *ns* AO probably contributes more to antibonding, while the lower-energy $(n - 1)d_{z^2}$ AO contributes more to bonding. For simplicity, the following MO scheme assumes the *ns* AO on the metal forms an essentially nonbonding σ^n level, leaving the $(n - 1)d_{z^2}$ AO to form bonding and antibonding MOs without showing possible *s-d* mixing.

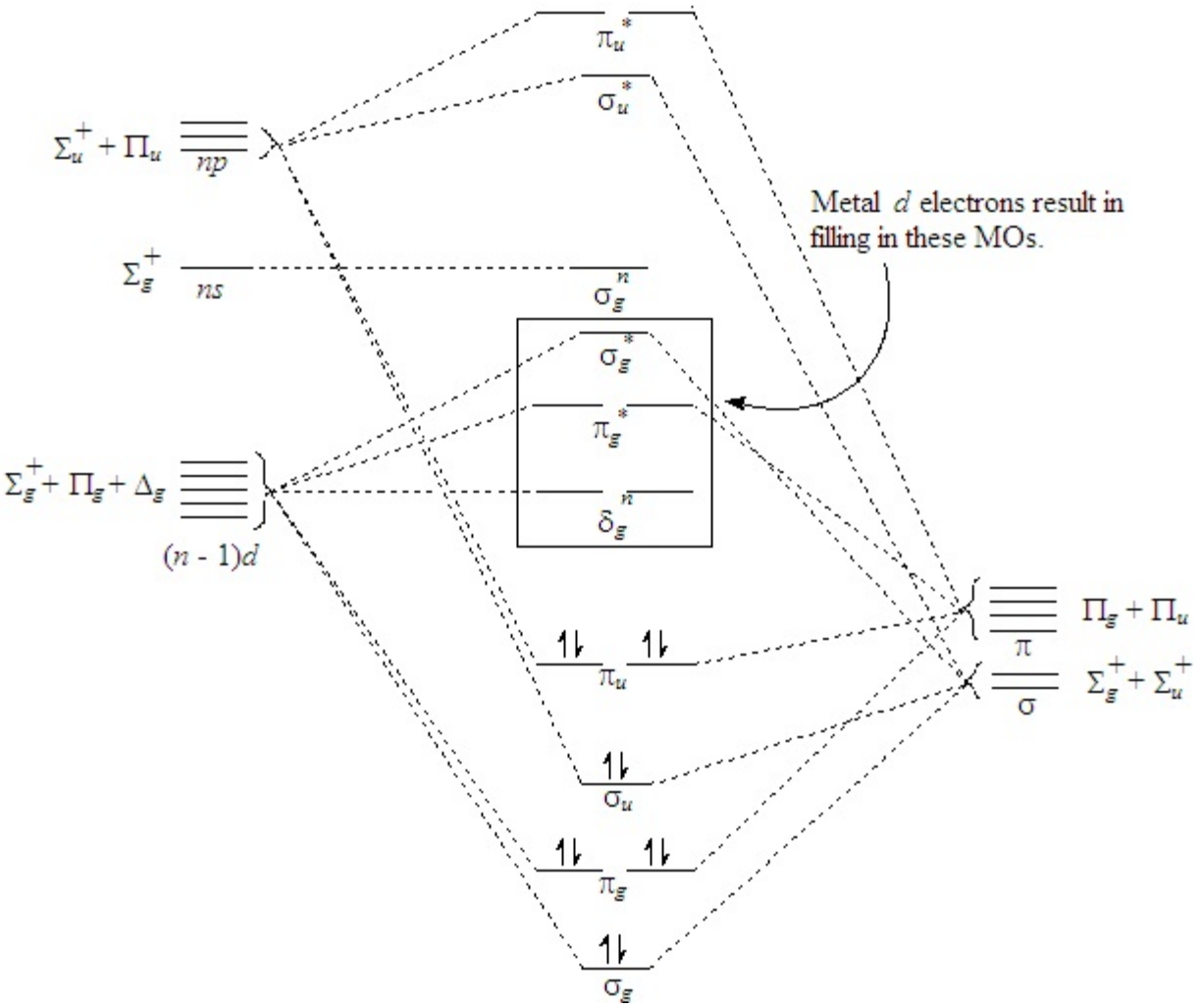

The MOs in the box have the same symmetry and splitting as the presumed splitting of *d* orbitals in the CFT model (cf. problem 7.2 a). Electron pairs contributed by ligands are sufficient to fill all lower levels. Therefore, any electrons contributed by the metal ion result in filling in the upper three levels in the same manner as predicted in the CFT model.

7.12 (a) For σ-SALCs, use the following four-vector basis set to obtain the reducible representation.

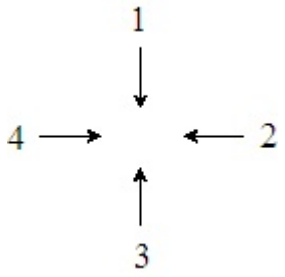

D_{4h}	E	$2C_4$	C_2	$2C_2'$	$2C_2''$	i	$2S_4$	σ_h	$2\sigma_v$	$2\sigma_d$
Γ_σ	4	0	0	2	0	0	0	4	2	0

$$\Gamma_\sigma = A_{1g} + B_{1g} + E_u$$

For π-SALCs, use the following eight-vector basis set to obtain the reducible representation.

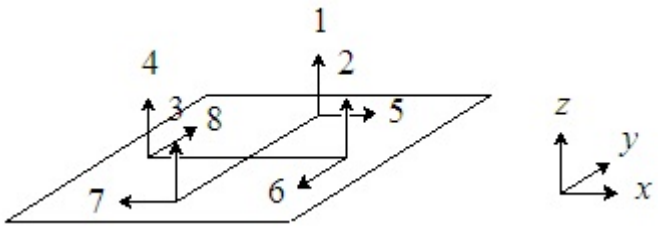

D_{4h}	E	$2C_4$	C_2	$2C_2'$	$2C_2''$	i	$2S_4$	σ_h	$2\sigma_v$	$2\sigma_d$
Γ_π	8	0	0	-4	0	0	0	0	0	0

$$\Gamma_\pi = A_{2g} + B_{2g} + E_g + A_{2u} + B_{2u} + E_u$$

(b) The matches between SALCs and central-atom AOs is shown below. Among the π-SALCs, A_{2g} and B_{2u} have no matching AOs and must be nonbonding (n.b.).

σ-SALCs	A_{1g}	B_{1g}	E_u
AOs	s, d_{z^2}	$d_{x^2-y^2}$	(p_x, p_y)

π-SALCs	A_{2g}	B_{2g}	E_g	A_{2u}	B_{2u}	E_u
AOs	n.b.	d_{xy}	(d_{xz}, d_{yz})	p_z	n.b.	(p_x, p_y)

(c) σ-SALCs:

$$\Sigma(A_{1g}) = \tfrac{1}{2}(\sigma_1 + \sigma_2 + \sigma_3 + \sigma_4)$$

$$\Sigma(B_{1g}) = \tfrac{1}{2}(\sigma_1 - \sigma_2 + \sigma_3 - \sigma_4)$$

$$\Sigma^{\alpha}(E_u) = 1/\sqrt{2}(\sigma_1 - \sigma_3)$$

$$\Sigma^{\beta}(E_u) = 1/\sqrt{2}(\sigma_2 - \sigma_4)$$

π-SALCs:

$$\Pi(A_{2g}) = \tfrac{1}{2}(\pi_5 + \pi_6 - \pi_7 - \pi_8) \qquad \text{(nonbonding)}$$

$$\Pi(B_{2g}) = \tfrac{1}{2}(\pi_5 - \pi_6 + \pi_7 + \pi_8)$$

$$\Pi^{\alpha}(E_g) = 1/\sqrt{2}(\pi_2 - \pi_4)$$

$$\Pi^{\beta}(E_g) = 1/\sqrt{2}(\pi_1 - \pi_3)$$

$$\Pi(A_{2u}) = \tfrac{1}{2}(\pi_1 + \pi_2 + \pi_3 + \pi_4)$$

$$\Pi(B_{2u}) = \tfrac{1}{2}(\pi_1 - \pi_2 + \pi_3 - \pi_4) \qquad \text{(nonbonding)}$$

$$\Pi^{\alpha}(E_u) = 1/\sqrt{2}(\pi_6 + \pi_8)$$

$$\Pi^{\beta}(E_u) = 1/\sqrt{2}(\pi_5 + \pi_7)$$

(d) $\Sigma(A_{1g}) + s$

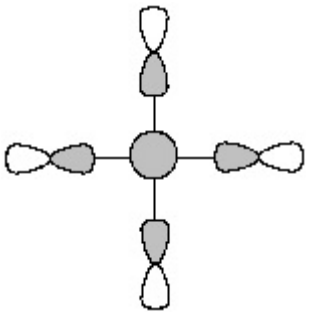

$\Sigma(A_{1g}) + d_{z^2}$

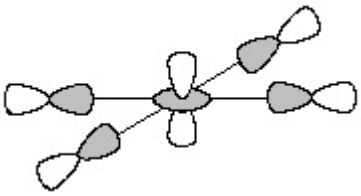

$\Sigma(B_{1g}) + d_{x^2-y^2}$

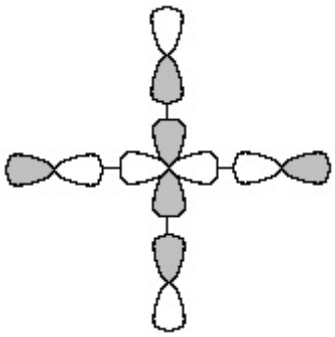

$\Sigma^{\alpha}(E_u) + p_y$; $\Sigma^{\beta}(E_u) + p_x$

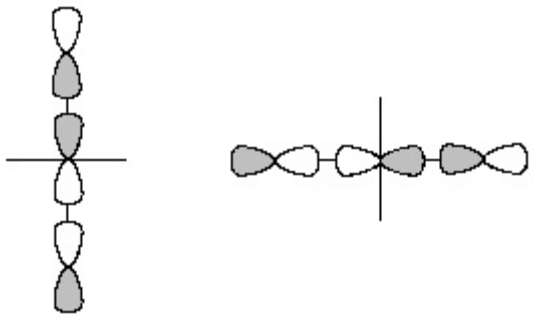

$\Pi(A_{2g})$

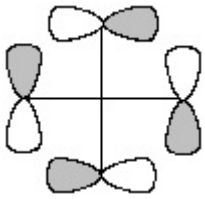

$\Pi(B_{2g}) + d_{xy}$

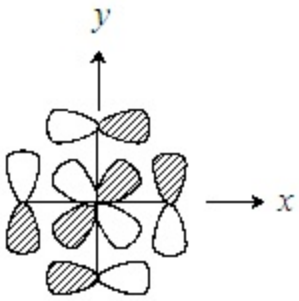

$\Pi^{\alpha}(E_g) + d_{xz}$; $\Pi^{\beta}(E_g) + d_{yz}$

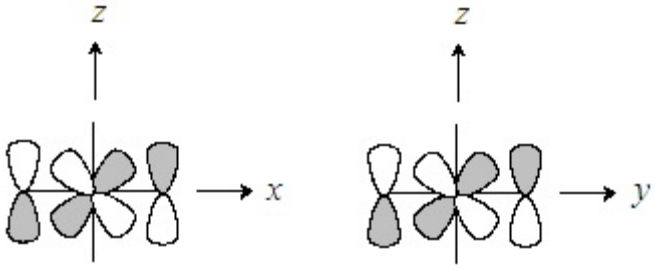

$\Pi(A_{2u}) + p_z$

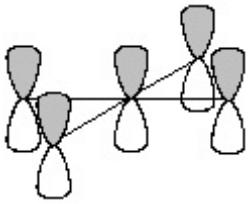

$\Pi(B_{2u})$

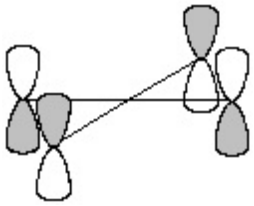

$\Pi^{\alpha}(E_u) + p_x$; $\Pi^{\beta}(E_u) + p_y$

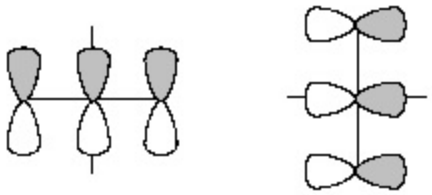

7.13 We can save labor by doing the work in *O* and then correlating to the matching *gerade* species of O_h, simply adding *g* subscripts to the Mulliken symbols in *O*.

For *G*, $L = 4$.

$\chi(E) = 2l + 1 = 9$

$\chi(C_3) = \{\sin (4.5)(120^o)\}/\{\sin 60^o\} = 0/0.866 = 0$

$\chi(C_2) = \{\sin (4.5)(180^o)\}/\{\sin 90^o\} = 1/1 = 1$

$\chi(C_4) = \{\sin (4.5)(90^o)\}/\{\sin 45^o\} = 0.707/0.707 = 1$

O	E	$8C_3$	$3C_2$	$6C_4$	$6C_2'$
Γ_G	9	0	1	1	1

$$\Gamma_G = A_{1g} + E_g + T_{1g} + T_{2g}$$

For *H*, $L = 5$.

$\chi(E) = 2l + 1 = 11$

$\chi(C_3) = \{\sin (5.5)(120^o)\}/\{\sin 60^o\} = -0.866/0.866 = -1$

$\chi(C_2) = \{\sin (5.5)(180^o)\}/\{\sin 90^o\} = -1/1 = -1$

$\chi(C_4) = \{\sin (5.5)(90^o)\}/\{\sin 45^o\} = 0.707/0.707 = 1$

O	E	$8C_3$	$3C_2$	$6C_4$	$6C_2'$
Γ_H	11	-1	-1	1	-1

$$\Gamma_H = E_g + 2T_{1g} + T_{2g}$$

For *I*, $L = 6$.

$\chi(E) = 2l + 1 = 13$

$\chi(C_3) = \{\sin (6.5)(120^o)\}/\{\sin 60^o\} = 0.866/0.866 = 1$

$\chi(C_2) = \{\sin (6.5)(180^o)\}/\{\sin 90^o\} = 1/1 = 1$

$\chi(C_4) = \{\sin (6.5)(90^o)\}/\{\sin 45^o\} = -0.707/0.707 = -1$

O	E	$8C_3$	$3C_2$	$6C_4$	$6C_2'$
Γ_I	13	1	1	-1	1

$$\Gamma_I = A_{1g} + A_{2g} + E_g + T_{1g} + 2T_{2g}$$

The splitting of *g* and *i* orbitals would be the same as the states, because both are *gerade*. The *h* orbitals are *ungerade*, and contrary to the *H* state will split as $e_u + 2t_{1u} + t_{2u}$.

7.14 (a) Use the $O_h \rightarrow D_{4h}$ correlation table.

Free-Ion Terms	Terms in O_h	Terms in D_{4h}
S	A_{1g}	A_{1g}
P	T_{1g}	$A_{2g} + E_g$
D	$E_g + T_{2g}$	$A_{1g} + B_{1g} + B_{2g} + E_g$
F	$A_{2g} + T_{1g} + T_{2g}$	$A_{2g} + B_{1g} + B_{2g} + 2E_g$
G	$A_{1g} + E_g + T_{1g} + T_{2g}$	$2A_{1g} + A_{2g} + B_{1g} + B_{2g} + 2E_g$
H	$E_g + 2T_{1g} + T_{2g}$	$A_{1g} + 2A_{2g} + B_{1g} + B_{2g} + 3E_g$
I	$A_{1g} + A_{1g} + E_g + T_{1g} + 2T_{2g}$	$2A_{1g} + A_{2g} + 2B_{1g} + 2B_{2g} + 3E_g$

(b) The most direct correlation for terms *S* through *F* is to use the R_3 correlation table showing $R_3 \rightarrow D_3$. For the *I* terms, use $O_h \rightarrow D_{3d}$ and then $D_{3d} \rightarrow D_3$.

Free-Ion Terms	Terms in O_h	Terms in D_3
S	A_{1g}	A_1
P	T_{1g}	$A_2 + E$
D	$E_g + T_{2g}$	$A_1 + 2E$
F	$A_{2g} + T_{1g} + T_{2g}$	$A_1 + 2A_2 + 2E$
G	$A_{1g} + E_g + T_{1g} + T_{2g}$	$2A_1 + A_2 + 3E$
H	$E_g + 2T_{1g} + T_{2g}$	$A_1 + 2A_2 + 4E$
I	$A_{1g} + A_{1g} + E_g + T_{1g} + 2T_{2g}$	$3A_1 + 2A_2 + 4E$

(c) There is no correlation table for $O_h \rightarrow D_{2d}$. Use results in part (a) with the table for $D_{4h} \rightarrow D_{2d}$ ($C_2' \rightarrow C_2'$). Note that for D_{2d}, the ligand-field terms are the same as for D_{4h} without the subscript g. Alternately, one could use the correlation $T_d \rightarrow D_{2d}$.

Free-Ion Terms	Terms in D_{4h}	Terms in D_{2d}
S	A_{1g}	A_1
P	$A_{2g} + E_g$	$A_2 + E$
D	$A_{1g} + B_{1g} + B_{2g} + E_g$	$A_1 + B_1 + B_2 + E$
F	$A_{2g} + B_{1g} + B_{2g} + 2E_g$	$A_2 + B_1 + B_2 + 2E$
G	$2A_{1g} + A_{2g} + B_{1g} + B_{2g} + 2E_g$	$2A_1 + A_2 + B_1 + B_2 + 2E$
H	$A_{1g} + 2A_{2g} + B_{1g} + B_{2g} + 3E_g$	$A_1 + 2A_2 + B_1 + B_2 + 3E$
I	$2A_{1g} + A_{2g} + 2B_{1g} + 2B_{2g} + 3E_g$	$2A_1 + A_2 + 2B_1 + 2B_2 + 3E$

(d) One the basis of vector transformations, determine the correlation between D_{4h} and $D_{\infty h}$, as follows:

D_{4h}	$D_{\infty h}$	Basis
A_{1g}	Σ_g^+	z^2
A_{2g}	Σ_g^-	R_z
$B_{1g} + B_{2g}$	Δ_g	$(x^2 - y^2, xy)$
E_g	Π_g	(R_x, R_y) (xz, yz)

Free-Ion Terms	Terms in D_{4h}	Terms in $D_{\infty h}$
S	A_{1g}	Σ_g^+
P	$A_{2g} + E_g$	$\Sigma_g^- + \Pi_g$
D	$A_{1g} + B_{1g} + B_{2g} + E_g$	$\Sigma_g^+ + \Pi_g + \Delta_g$
F	$A_{2g} + B_{1g} + B_{2g} + 2E_g$	$\Sigma_g^- + 2\,\Pi_g + \Delta_g$
G	$2A_{1g} + A_{2g} + B_{1g} + B_{2g} + 2E_g$	$2\Sigma_g^+ + \Sigma_g^- + 2\Pi_g + \Delta_g$
H	$A_{1g} + 2A_{2g} + B_{1g} + B_{2g} + 3E_g$	$\Sigma_g^+ + 2\Sigma_g^- + 3\Pi_g + \Delta_g$
I	$2A_{1g} + A_{2g} + 2B_{1g} + 2B_{2g} + 3E_g$	$2\Sigma_g^+ + \Sigma_g^- + 3\Pi_g + 2\Delta_g$

7.15 (a) There are four microstates:

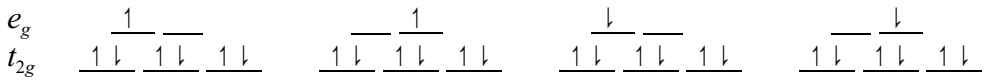

(b) Use Table 7.2, or apply Eqs. (7.2) - (7.6) for $L = 4$. Either way, the states emerging from ^2G are $^2A_{1g}$, ^2E_g, $^2T_{1g}$, $^2T_{2g}$.

(c) For ^2G, $D_t = (2)(9) = 18$.
For $^2A_{1g} + {}^2E_g + {}^2T_{1g} + {}^2T_{2g}$, $D_t = (2)(1) + (2)(2) + (2)(3) + (2)(3) = 18$.

7.16 The free-ion terms of d^n and d^{10-n} are the same because they arise from the same number of microstates, as shown by Eq. (7.14):

$$D_t(n) = \frac{10!}{(10 - n)!n!}$$

$$D_t(10 - n) = \frac{10!}{[10 - (10 - n)]!(10 - n)!} = \frac{10!}{n!(10 - n)!}$$

The free-ion terms are unique to a given number of microstates. Moreover, each free-ion term splits into a characteristic set of ligand-field terms in any point group. Thus, the ligand-field terms for d^n and d^{10-n} must be the same.

7.17 The strong-field terms emerging from the $d^2\ T_d$ configurations in the hypothetical extreme field are the same as for the comparable $d^2\ O_h$ configurations, except that the subscript g is omitted for each. The extreme-field configurations, however, will be in the reverse energy order of the $d^2\ O_h$ configurations; i.e., $e^2 < e^1t_2^1 < t_2^2$. Identifying the triplet terms versus the singlet terms follows the same logic as shown in the $d^2\ O_h$ case; i.e., each configuration gives rise to the same multiplicities for comparable T_d orbital terms. Making the correlations in the same way gives a diagram identical to that shown for $d^8\ O_h$ (Fig. 7.26), except for the *gerade* designations on the states.

7.18 *Weak-Field Terms.* In O_h, the free-ion ^2D term of a d^9 configuration becomes a ^2E_g ground state term and a $^2T_{2g}$ excited state terms. From the correlation tables, it can be seen that these terms split on descent to D_{4h} square planar geometry as follows:

$$^2E_g \rightarrow {}^2A_{1g} + {}^2B_{1g} \qquad {}^2T_{2g} \rightarrow {}^2B_{2g} + E_g$$

Extreme Field Configurations and Strong-Field Terms. The configurations for the $d^9\ D_{4h}$ square planar geometry in an extremely strong field are shown below in order of increasing energy. The terms in a strong field are obtained by taking the orbital assignment of the unpaired electron as a basis for a representation in D_{4h}. All paired electrons can be ignored, because the representation for any pair must be the totally symmetric representation; e.g., $B_{1g} \times B_{1g} = A_{1g}$. With only one unpaired electron in all configurations, all terms must be doublets.

b_{1g}	$\underline{\uparrow}$	$\underline{\uparrow\downarrow}$	$\underline{\uparrow\downarrow}$	$\underline{\uparrow\downarrow}$
b_{2g}	$\underline{\uparrow\downarrow}$	$\underline{\uparrow}$	$\underline{\uparrow\downarrow}$	$\underline{\uparrow\downarrow}$
a_{1g}	$\underline{\uparrow\downarrow}$	$\underline{\uparrow\downarrow}$	$\underline{\uparrow}$	$\underline{\uparrow\downarrow}$
e_g	$\underline{\uparrow\downarrow}\ \underline{\uparrow\downarrow}$	$\underline{\uparrow\downarrow}\ \underline{\uparrow\downarrow}$	$\underline{\uparrow\downarrow}\ \underline{\uparrow\downarrow}$	$\underline{\uparrow\downarrow}\ \underline{\uparrow}$
	$^2B_{1g}$	$^2B_{2g}$	$^2A_{1g}$	^2E_g

The resulting qualitative correlation diagram is shown below.

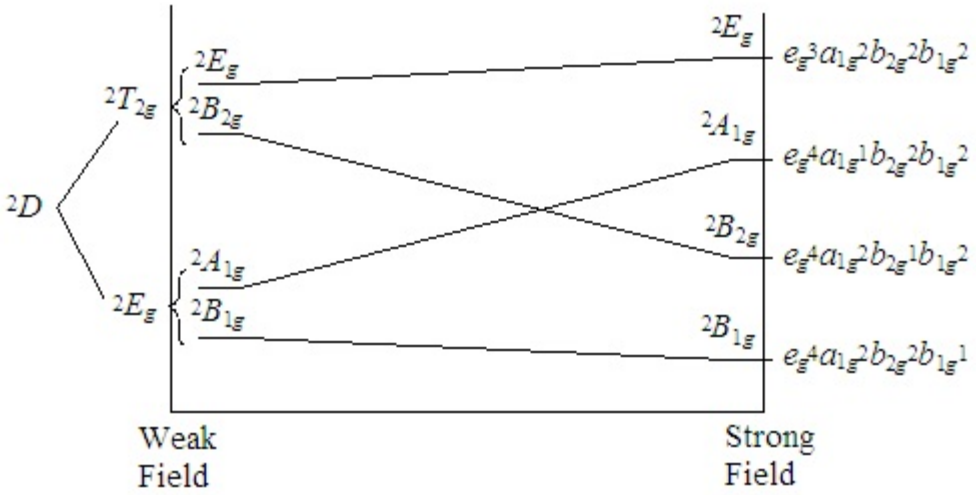

7.19 (a) FeF_6^{3-} is a d^5 high-spin complex, because F^- is a weak-field ligand. Therefore, there are no spin-allowed transitions from the ${}^6A_{1g}$ ground state. $Fe(CN)_6^{3-}$ is a d^5 low-spin complex, because CN^- is a strong-field ligand. The ground state is ${}^2T_{2g}$ term. From the Tanabe-Sugano diagram for d^5 low-spin cases (right side), it is apparent that there are at least three possible spin allowed transitions: ${}^2T_{2g} \rightarrow [{}^2A_{2g}, {}^2T_{1g}]$, ${}^2T_{2g} \rightarrow {}^2E_g$, ${}^2T_{2g} \rightarrow {}^2A_{2g}$. As the Tanabe-Sugano diagram indicates, the ${}^2A_{2g}$ and ${}^2T_{1g}$ states for the first transition are virtually degenerate and would give rise to a single broad band. These transitions account for the color of $Fe(CN)_6^{3-}$.

(b) Tetrahedral complexes are not centrosymmetric, so the LaPorte Rule does not apply. Nonetheless, *d* orbitals have an inherent *gerade* character. Therefore, although molar absorptivities are slightly higher for tetrahedral complexes compared to octahedral complexes, they are still relatively low by comparison to charge-transfer transitions.

(c) {The charge on the complex should be 3+, not 2+ as shown in the first printing.} $[Cr(H_2O)_3]^{3+}$ is an octahedral d^3 case. From either the Tanabe-Sugano diagram or Orgel diagram, three bands are expected from the transitions ${}^4A_{2g} \rightarrow {}^4T_{2g}$, ${}^4A_{2g} \rightarrow {}^4T_{1g}(F)$, ${}^4A_{2g} \rightarrow {}^4T_{1g}(P)$. The last of these involves a change in configuration from $t_{2g}{}^3$ to $t_{2g}{}^1e_g{}^2$; i.e., a two-electron transition. This is a less probable event and therefore would have a lower absorptivity. Moreover, it is the highest energy transition and may be obscured by the tail of a stronger charge-transfer band in the ultraviolet.

(d) A d^6 high-spin complex such as $[Fe(H_2O)_6]^{2+}$ is expected to show a single band from the transition ${}^5T_{2g} \rightarrow {}^5E_g$. However, both the ground state and excited state are degenerate and subject to Jahn-Teller distortions. The distortion is greater for the doubly degenerate excited state. Therefore, the observed band splitting is primarily due to lifting of the degeneracy of the upper ${}^5E_g$ state.

(e) With d^0 configurations, both complex ions have no possible *d*-*d* transitions. The observed intense colors arise from L→M charge transfer transitions, which are LaPorte allowed. Such transitions can have very high molar absorptivities.

7.20 (a) Use direct products for the configurations to determine the orbital term designations. Where two electrons are paired in the same orbital the product is totally symmetric. The ground state $e_g{}^4a_{1g}{}^2b_{2g}{}^2$ consists of all paired electrons, so the term is ${}^1A_{1g}$. For the first excited singlet state $e_g{}^4a_{1g}{}^2b_{2g}{}^1b_{1g}{}^1$, take the direct product $B_{2g} \times B_{1g}$:

D_{4h}	E	$2C_4$	C_2	$2C_2'$	$2C_2''$	i	$2S_4$	σ_h	$2\sigma_v$	$2\sigma_v$
B_{2g}	1	-1	1	-1	1	1	-1	1	-1	1
B_{1g}	1	-1	1	1	-1	1	-1	1	1	-1
$\Gamma = A_{2g}$	1	1	1	-1	-1	1	1	1	-1	-1

Therefore, the first singlet excited state is $^1A_{2g}$. For the second excited singlet state $e_g^{\,4}a_{1g}^{\,1}b_{2g}^{\,2}b_{1g}^{\,1}$ the direct product is $A_{1g} \times B_{1g} = B_{1g}$, and the resulting term is $^1B_{1g}$. For the third excited singlet state $e_g^{\,3}a_{1g}^{\,2}b_{2g}^{\,2}b_{1g}^{\,1}$, the direct product is $E_g \times B_{1g}$:

D_{4h}	E	$2C_4$	C_2	$2C_2'$	$2C_2''$	i	$2S_4$	σ_h	$2\sigma_v$	$2\sigma_v$
E_g	2	0	-2	0	0	2	0	-2	0	0
B_{1g}	1	-1	1	1	-1	1	-1	1	1	-1
$\Gamma = E_g$	2	0	-2	0	0	2	0	-2	0	0

Therefore the term is ^1E_g.

(b) The three electronic transitions are

$$^1A_{1g} \rightarrow {}^1A_{2g}$$
$$^1A_{1g} \rightarrow {}^1B_{1g}$$
$$^1A_{1g} \rightarrow {}^1E_g$$

(c) For an electronic transition to be vibronically allowed, the transition moment $\int \psi_e \psi_v \mu \psi_e' \psi_v' \, d\tau$ must be totally symmetric to be non-zero. In this specific case ψ_e is also totally symmetric, and the ground vibrational state, ψ_v is totally symmetric for all molecules except free radicals. Therefore the symmetry of the integral depends upon the symmetries of the direct products $\mu \times \psi_e' \times \psi_v'$. The symmetries of the dipole moment components, obtained from the unit vector transformation properties listed in the D_{4h} character table are

$$\mu_z = A_{2u} \qquad (\mu_x, \mu_y) = E_u$$

The symmetries of the excited electronic states, as shown in part (a), are A_{2g}, B_{1g}, and E_g. The symmetries of the components of μ are *ungerade*, and the symmetries of the electronic excited states are *gerade*, so the products $\mu \times \psi_e'$ must all be *ungerade*. In order for the integral to be totally symmetric and nonvanishing, the ψ_v' must belong to an identical *ungerade* species as $\mu \times \psi_e'$. The *ungerade* normal modes of vibration, which might couple with the electronic transitions, are

$$\nu_3 \, (A_{2u}) \qquad \nu_5 \, (B_{2u}) \qquad \nu_6 \, (E_u) \qquad \nu_7 (E_u)$$

For the purpose of vibronic coupling, the *gerade* normal modes can be ignored. By matching symmetries of $\mu \times \psi_e'$ with one or more of these ψ_v' we obtain the following results, which show the normal modes that vibronically allow each electronic transition:

Transition	$\mu \times \psi_e'$	Matching normal modes
$^1A_{1g} \rightarrow {}^1A_{2g}$	$A_{2u} \times A_{2g} = A_{1u}$	none
	$E_u \times A_{2g} = E_u$	ν_6, ν_7 (E_u)
$^1A_{1g} \rightarrow {}^1B_{1g}$	$A_{2u} \times B_{1g} = B_{2u}$	ν_5 (B_{2u})
	$E_u \times B_{1g} = E_u$	ν_6, ν_7 (E_u)
$^1A_{1g} \rightarrow {}^1E_g$	$A_{2u} \times E_g = E_u$	ν_6, ν_7 (E_u)
	$E_u \times E_g = A_{1u} + A_{2u} + B_{1u} + B_{2u}$	ν_3 (A_{2u}), ν_5 (B_{2u})

In the first case for $^1A_{1g} \rightarrow {}^1A_{2g}$, the integral with the dipole moment component μ_z (A_{2u}) vanishes, because there is no matching normal mode with the resultant A_{1u} symmetry. Nonetheless, the transition $^1A_{1g} \rightarrow {}^1A_{2g}$ is vibronically allowed by coupling with the normal modes ν_6 and ν_7 (E_u), because the direct product $\mu \times \psi_e'$ with the degenerate pair of dipole moment components (μ_x, μ_y) is E_u, making the full integral totally symmetric. In the last case for $^1A_{1g} \rightarrow {}^1E_g$, the direct product $E_u \times E_g$ is a reducible representation, only two whose component irreducible representations (A_{2u} and B_{2u}) match symmetries with normal modes. Those matches are sufficient to vibronically allow the $^1A_{1g} \rightarrow {}^1E_g$ electronic transition.